SAE 41B17M
(PS 19) Carburized Case (ATM) Steel
Iteration #73

Microstructural Data, Monotonic and Fatigue Test Results

Prepared by:

N. Cyril
and
A. Fatemi

Department of Mechanical, Industrial and Manufacturing Engineering
The University of Toledo
Toledo, Ohio 43606

Prepared for:
The AISI Bar Steel Applications Group

January 2008

American Iron and Steel Institute
2000 Town Center, Suite 320
Southfield, Michigan 48075
tel: 248-945-4777
fax: 248-352-1740
www.autosteel.org

TABLE OF CONTENTS

NOMENCLATURE

A_o, A_f	initial, final area	S	engineering stress
HB, HRB, HRC	Brinell, Rockwell B-Scale, Rockwell C-Scale hardness number	YS, UYS, LYS, YS'	monotonic yield, upper yield, lower yield, cyclic yield strength
b, c, n	fatigue strength, fatigue ductility, strain hardening exponent	YPE	yield point elongation
D_o, D_f	initial, final diameter	S_u	ultimate tensile strength
e	engineering strain	%EL	percent elongation
E, E'	monotonic, midlife cycle modulus of elasticity	%RA	percent reduction in area
K, K'	monotonic, cyclic strength coefficient	σ, σ_f, σ_f'	true stress, true fracture strength, fatigue strength coefficient
L_o, L_f	initial, final gage length	σ_a, σ_m, $\Delta\sigma$	stress amplitude, mean stress, stress range
$N_{50\%}$, $(N_f)_{10\%}$, $(N_f)_{50\%}$,	number of cycles to midlife, 10% load drop, 50% load drop	ε_e, ε_p, ε	true elastic, plastic, total strain
$2N_f$	reversals to failure	ε_f, ε_f'	true fracture ductility, fatigue ductility coefficient
P_f, P_u	fracture, ultimate load	ε_a, ε_m, $\Delta\varepsilon$	strain amplitude, mean strain, strain range
R	neck radius; or strain ratio	$\Delta\varepsilon_e$, $\Delta\varepsilon_p$	elastic, plastic strain range

UNIT CONVERSION TABLE

Measure	SI Unit	US Unit	from SI to US	from US to SI
Length	mm	in	1 mm = 0.03937 in	1 in = 25.4 mm
Area	mm^2	in^2	1 mm^2 = 0.00155 in^2	1 in^2 = 645.16 mm^2
Load	kN	klb	1kN = 0.2248 klb	1 klb = 4.448 kN
Stress	MPa	ksi	1 MPa = 0.14503 ksi	1 ksi = 6.895 MPa
Temperature	°C	°F	°C = (°F - 32)/1.8	°F = (°C * 1.8) + 32

In SI Unit:	1 kN = 10^3 N	1 Pa = 1 N/m^2	1 MPa = 10^6 Pa = 1 N/mm^2	1 Gpa = 10^9 Pa
In US Unit:	1 klb = 10^3 lb	1 psi = 1 lb/in^2	1 ksi = 10^3 psi	

SUMMARY

The micro structural data, monotonic properties, and fatigue behavior data have been obtained for SAE 41B17M (PS19) Carburized Case (Atm) steel. The material was provided for the American Iron and Steel Institute (AISI) by Timken Company. Micro structural data includes grain type, grain size, and inclusion content. The desired monotonic properties were acquired from one tensile test. Fourteen strain-controlled fatigue tests were used to generate the strain-life and cyclic stress-strain curves and properties. The experimental procedure followed and results obtained are presented and discussed in this report.

I. EXPERIMENTAL PROGRAM

1.1 Material and Specimen Fabrication

1.1.1 Material

The SAE 41B17M (PS 19) Carburized Case (Atm) steel was provided by Timken Company as round bars. The specimens were machined at the University of Toledo. In Table 1, the chemical composition supplied by Timken Company is shown.

1.1.2 Specimen

In this study, identical round specimens were used for the monotonic and fatigue tests. The specimen configuration and dimensions are shown in Figure 1. This configuration deviates slightly from the specimens recommended by ASTM Standard E606 [1]. The recommended specimens have uniform or hourglass test sections. The specimen geometry shown in Figure 1 differs by using a large secondary radius throughout the test section.

All specimens were machined in the Mechanical, Industrial, and Manufacturing Engineering Machine Shop at the University of Toledo. The specimens were initially turned on a lathe to an appropriate diameter for insertion into a CNC machine. Using the CNC machine, final turning was performed to achieve the tolerable dimensions slightly larger than those specified on the specimen drawings. The specimens were then ground at a commercial machine shop to obtain the specified dimensions.

A commercial round-specimen polishing machine was used to polish the specimen gage section after grinding. Three different grits of aluminum oxide lapping film were used: 30μ, 12μ,

and 3μ. The 3μ grit was used as the final polish and polishing marks coincided with the specimens' longitudinal direction. The polished surfaces were carefully examined under magnification to ensure complete removal of machine marks within the test section.

After polishing the specimens were heat treated at DaimlerChrysler Corporation. Subsequent to heat treatment, specimens were then tested with the as received surface condition. Slight bending of specimens caused due to heat-treatment did not seem to have an influence on test results. Table 2 summarizes the bending measured and the test results.

1.2 Testing Equipment

1.2.1 Apparatus

An MTS closed-loop servo-controlled hydraulic axial load frame in conjunction with a Fast-Track digital servo-controller was used to conduct the tests. The calibration of this system was verified prior to beginning the test program. The load cell used had a capacity of 100 kN. Hydraulically operated grips using universal tapered collets were employed to secure the specimens' ends in series with the load cell.

Total strain was controlled for all tests using an extensometer rated as ASTM class B1 [2]. The calibration of the extensometer was verified using displacement apparatus containing a micrometer barrel in divisions of 0.0001 in. The extensometer had a gage length of 0.30 in and was capable of measuring strains up to 15 %.

In order to protect the specimens' surface from the knife-edges of the extensometer, ASTM Standard E606 recommends the use of transparent tape or epoxy to 'cushion' the attachment. For this study, it was found that application of transparent tape strips was difficult

due to the radius within the test section. Therefore, epoxy was considered to be the best protection. One disadvantage of epoxy is the variability of mixtures throughout the test program. As an alternative to epoxy, M-coat D offered a more consistent mixture. Therefore, the tests were performed using M-coat D.

1.2.2 Alignment

Significant effort was put forth to align the load train (load cell, grips, specimen, and actuator). Misalignment can result from both tilt and offset between the central lines of the load train components. According to ASTM Standard E606, the maximum bending strains should not exceed 5% of the minimum axial strain range imposed during any test program. For this study, the minimum axial strain range was 0.004 in/in, which was used in the run-out fatigue tests. Therefore, the maximum allowable bending strain was 200 microstrain. ASTM Standard E1012, Type A, Method 1 was followed to verify specimen alignment [3]. For this procedure, two arrays of four strain gages per array were arranged at the upper and lower ends of the uniform gage section. For each array, gages were equally spaced around the circumference of a 0.5-in. diameter specimen with uniform gage section. The maximum bending strain determined from the gaged specimen was within the allowable ASTM limit.

1.3 Test Methods and Procedures

1.3.1 Monotonic tension tests

The monotonic test in this study was performed using test methods specified by ASTM Standard E8 [4]. Strain control was used.

For the elastic and initial yield region (0% to 0.5% strain), a strain rate of 0.0012 in/in/min was chosen. This strain rate was one half of the maximum allowable rate specified by ASTM Standard E8 for the initial yield region. Due to the high brittleness of the material, the same rate was used after yielding as well.

After the tension test was concluded, the broken specimens were carefully reassembled. The final gage length of the fractured specimen was measured with a Vernier caliper having divisions of 0.001 in. Using an optical comparator with 10X magnification and divisions of 0.001 in, the final diameter was measured. It should be noted that prior to the test, the initial minimum diameter was measured with this same instrument.

1.3.2 Constant amplitude fatigue tests

All constant amplitude fatigue tests in this study were performed according to ASTM Standard E606. It is recommended by this standard that at least 10 specimens be used to generate the fatigue properties. For this study, 14 specimens at 6 different strain amplitudes ranging from 0.2% to 0.65% were utilized. Several additional samples were tested. However, due to pre-mature failure, these did not yield valid tests (see Table 2). INSTRON LCF software was used in all strain-controlled tests. During each strain-controlled test, the total strain was recorded using the extensometer output. Test data were automatically recorded throughout each test.

There were two control modes used for these tests. Strain control was used in all tests with plastic deformation. For some of the elastic tests, strain control was used initially to determine the stabilized load, then load control was used for the remainder of the test and for the rest of the elastic tests, load control was used throughout. The reason for the change in control mode was due to the frequency limitation on the extensometer. For the strain- controlled tests,

the applied frequencies was 0.2 Hz. For the load control tests, frequencies of up to 25 Hz were used in order to shorten the overall test duration. All tests were conducted using a triangular waveform.

II. Experimental results and analysis

2.1 Microstructural Data

Photomicrographs of the microstructure were obtained using an optical microscope with a digital camera attachment. In Figure 2, the microstructure in the plane perpendicular to applied load (L-T' direction) is shown. It can be seen from the photomicrograph that SAE 41B17M (PS 19) Carburized Case (Atm) steel has a martensite microstructure. In Figure 3, the inclusions in the plane perpendicular to the applied load (L-T') and T-T' are shown.

The average grain size was measured in both transverse and longitudinal directions using the Linear Intercept Procedures reported in ASTM Standard E112 [5]. According to ASTM Standard E45, method A, the inclusion rating numbers for type A inclusion were found [6]. Rockwell hardness tests were also performed. A summary of the microstructural data for SAE 41B17M (PS 19) Carburized Case (Atm) steel is provided in Table 3.

2.2 Monotonic Deformation Behavior

The properties determined from monotonic tests were the following: modulus of elasticity (E), yield strength (YS), ultimate tensile strength (S_u), percent elongation (%EL), percent reduction in area (%RA), true fracture strength (σ_f), true fracture ductility (ε_f), strength coefficient (K), and strain hardening exponent (n).

True stress (σ), true strain (ε), and true plastic strain (ε_p) were calculated from engineering stress (S) and engineering strain (e), according to the following relationships which are based on constant volume assumption:

$$\sigma = S(1+e) \tag{1a}$$

$$\varepsilon = \ln(1+e) \tag{1b}$$

$$\varepsilon_p = \varepsilon - \varepsilon_e = \varepsilon - \frac{\sigma}{E} \tag{1c}$$

The true stress (σ) - true strain (ε) plot is often represented by the Ramberg-Osgood equation:

$$\varepsilon = \varepsilon_e + \varepsilon_p = \frac{\sigma}{E} + \left(\frac{\sigma}{K}\right)^{\frac{1}{n}} \tag{2}$$

The strength coefficient, K, and strain hardening exponent, n, are the intercept and slope of the best line fit to true stress (σ) versus true plastic strain (ε_p) data in log-log scale:

$$\sigma = K\left(\varepsilon_p\right)^n \tag{3}$$

In accordance with ASTM Standard E739 [7], when performing the least squares fit, the true plastic strain (ε_p) was the independent variable and the stress (σ) was the dependent variable. The plot for the test conducted is shown in Figure 4. Since the tension test in this material did not

last up to 0.2% plastic strain, the yield strength has been defined at the ultimate tensile strength. The points on the stress-strain curve which deviated from the straight line along the initial linear portion of the curve have been included in the fit for K and n values. Therefore, the valid data range occurred between the start of plastic deformation and the strain at maximum load.

The true fracture strength, σ_f, was calculated from:

$$\sigma_f = P_f / A_f \tag{4}$$

where P_f is the load at fracture and A_f is the area at fracture.

The true fracture ductility, ε_f, was calculated from the relationship based on constant volume:

$$\varepsilon_f = \ln\left(\frac{A_o}{A_f}\right) = \ln\left(\frac{1}{1 - RA}\right) \tag{5}$$

where A_f is the cross-sectional area at fracture, A_o is the original cross-sectional area, and RA is the reduction in area.

A summary of the monotonic properties for SAE 41B17M (PS 19) Carburized Case (Atm) steel is provided in Table 3. The monotonic stress-strain curve is shown in Figure 5. The curve for this material is compared with the corresponding curve for the same material at a similar hardness, heat-treated under a different condition (Vac 1800° F) in Figure 6. Refer to Table A.1 in the Appendix for a summary of the monotonic test results.

2.3 Cyclic Deformation Behavior

2.3.1 Transient cyclic response

Transient cyclic response describes the process of cyclic-induced change in deformation resistance of a material. Data obtained from constant amplitude strain-controlled fatigue tests were used to determine this response. Plots of stress amplitude variation versus applied number of cycles can indicate the degree of transient cyclic softening/hardening. Also, these plots show when cyclic stabilization occurs. A composite plot of the transient cyclic response for SAE 41B17M (PS 19) Carburized Case (Atm) steel is shown in Figure A.1 of the Appendix. The transient response was normalized on the rectangular plot in Figure A.1a, while a semi-log plot is shown in Figure A.1b. Even though multiple tests were conducted at each strain amplitude, data from one test at each strain amplitude tested are shown in these plots.

2.3.2 Steady-state cyclic deformation

Another cyclic behavior of interest was the steady state or stable response. Data obtained from constant amplitude strain-controlled fatigue tests were also used to determine this response. Due to the lack of sufficient plastic strain data for this material, the only property determined from the steady-state hysteresis loops was the cyclic modulus of elasticity (E'). The cyclic strength coefficient (K'), cyclic strain hardening exponent (n'), and cyclic yield strength (YS') could not be determined. Half-life (midlife) hysteresis loops and data were used to obtain the stable cyclic properties.

Similar to monotonic behavior, the cyclic true stress-strain behavior can be characterized by the Ramberg-Osgood type equation:

$$\frac{\Delta \varepsilon}{2} = \frac{\Delta \varepsilon_e}{2} + \frac{\Delta \varepsilon_p}{2} = \frac{\Delta \sigma}{2E} + \left(\frac{\Delta \sigma}{2K'} \right)^{\frac{1}{n'}} \quad (6)$$

It should be noted that in Equation 6 and the other equations that follow, E is the modulus of elasticity that was calculated from the monotonic test.

The cyclic strength coefficient, K', and cyclic strain hardening exponent, n', are the intercept and slope of the best line fit to true stress amplitude ($\Delta\sigma/2$) versus true plastic strain amplitude ($\Delta\varepsilon_p/2$) data in log-log scale:

$$\frac{\Delta \sigma}{2} = K' \left(\frac{\Delta \varepsilon_p}{2} \right)^{n'} \quad (7)$$

In accordance with ASTM Standard E739, when performing the least squares fit, the true plastic strain amplitude ($\Delta\varepsilon_p/2$) is the independent variable and the stress amplitude ($\Delta\sigma/2$) is the dependent variable. The true plastic strain amplitude is calculated by the following equation:

$$\frac{\Delta \varepsilon_p}{2} = \frac{\Delta \varepsilon}{2} - \frac{\Delta \sigma}{2E} \quad (8)$$

However, due to the high brittleness of this material, only one level of test data which included plastic deformation could be obtained for this material. Therefore, it was not possible to obtain this plot and the cyclic stress-strain curve.

Figure A.2 in the Appendix shows plots of the steady-state (midlife) hysteresis loops. The stable loops from the two tests that contained plastic deformation at a total strain amplitude of 0.65% are shown in these plots. It may be noted that the strength in tension is lower than that in compression and thus, resulting in a compressive mean stress for the fully reversed strain-controlled test performed.

2.4 Constant Amplitude Fatigue Behavior

Constant amplitude strain-controlled fatigue tests were performed to determine the strain-life curve. The following equation relates the true strain amplitude to the fatigue life:

$$\frac{\Delta\varepsilon}{2}=\frac{\Delta\varepsilon_e}{2}+\frac{\Delta\varepsilon_p}{2}=\frac{\sigma_f'}{E}(2N_f)^b+\varepsilon_f'(2N_f)^c \qquad (9)$$

where σ_f' is the fatigue strength coefficient, b is the fatigue strength exponent, ε_f' is the fatigue ductility coefficient, c is the fatigue ductility exponent, E is the monotonic modulus of elasticity, and $2N_f$ is the number of reversals to failure (which was defined as a 50% load drop, as recommended by ASTM Standard E606).

The fatigue strength coefficient, σ_f', and fatigue strength exponent, b, are the intercept and slope of the best line fit to true stress amplitude ($\Delta\sigma/2$) versus reversals to failure ($2N_f$) data in log-log scale:

$$\frac{\Delta\sigma}{2}=\sigma_f'(2N_f)^b \qquad (10)$$

In accordance with ASTM Standard E739, when performing the least squares fit, the stress amplitude ($\Delta\sigma/2$) was the independent variable and the reversals to failure ($2N_f$) was the dependent variable. This plot is shown in Figure 7. To generate the σ_f' and b values, the range of data used in this figure was chosen for $N_f \leq 10^5$ cycles. The curve for this material is compared with the corresponding curve for the same material at a similar hardness, heat-treated under a different condition (Vac 1800° F) in Figure 8.

The fatigue ductility coefficient, ε_f', and fatigue ductility exponent, c, are the intercept and slope of the best line fit to calculated true plastic strain amplitude ($\Delta\varepsilon_p/2$) versus reversals to failure ($2N_f$) data in log-log scale:

$$\left(\frac{\Delta\varepsilon_p}{2}\right)_{calculated} = \varepsilon_f'\left(2N_f\right)^c \qquad (11)$$

In accordance with ASTM Standard E739, when performing the least squares fit, the calculated true plastic strain amplitude ($\Delta\varepsilon_p/2$) is the independent variable and the reversals to failure ($2N_f$) was the dependent variable. The calculated true plastic strain amplitude was determined from Equation 8. It was not possible to generate this plot due to lack of sufficient plastic strain data.

The true strain amplitude versus reversals to failure plot is shown in Figure 9. This plot displays the strain - life curve (Eqn. 9) which is essentially the elastic strain portion (Eqn. 10), and superimposed fatigue data. A summary of the cyclic properties for SAE 41B17M (PS 19) Carburized Case (Atm) steel is provided in Table 3. Table A.2 in the Appendix provides the summary of the fatigue test results.

A parameter often used to characterize fatigue behavior at stress concentrations, such as at the root of a notch, is Neuber's parameter [10]. Neuber's stress range is given by:

$$\sqrt{(\Delta\varepsilon)(\Delta\sigma)E} = 2\sqrt{(\sigma_f')^2\left(2N_f\right)^{2b} + \sigma_f'\varepsilon_f' E\left(2N_f\right)^{b+c}} \qquad (12)$$

The Neuber's stress range versus reversals to failure could not be plotted as the fatigue ductility coefficient and exponent could not be determined.

Table 1: Chemical composition of SAE 41B17M (PS 19) Carburized Case (Atm) steel

Element	Wt. %
Carbon, C	0.1800%
Manganese, Mn	1.1300%
Phosphorus, P	0.0170%
Sulfur, S	0.0200%
Silicon, Si	0.2600%
Vanadium, V	0.0060%
Chromium, Cr	0.5200%
Aluminum, Al	0.0360%
Copper, Cu	0.1800%
Nickel, Ni	0.1200%
Molybdenum, Mo	0.1200%
Arsenic, As	0.0050%
Boron, B	0.0023%
Calcium, Ca	0.0003%
Cerium, Cb	0.0020%
Cobalt, Co	0.0080%
Nitrogen, N	0.0082%
Lead, Pb	0.0005%
Antimony, Sb	0.0020%
Tin, Sn	0.0080%
Titanium, Ti	0.0420%
Tungsten, W	0.0040%
Zirconium, Zr	0.0010%

Table 2: Summary of bending in specimens and the tests performed.

Spec - ID	Bending range (in.)	Test	Good test?, cycles to failure	Pre-mature failure load
73-1	0.003-0.004	0.2%	Yes, 87000	
73-2	0.002-0.003	0.5%	Yes, 505	
73-3	0.004-0.005	0.65%	Yes, 64	
73-4	0.003-0.004	0.3%	Yes, 6817	
73-5	0.002-0.003	0.5%	No	3200 lbs
73-6	0.004-0.005	0.3%	No	2000 lbs
73-7	0.005-0.006	0.225%	Yes, Run-out	
73-8	0.004-0.005		No	700 lbs
73-9	0.004-0.005	0.4%	Yes, 2702	
73-10	0.004-0.005	0.65%	No	3800 lbs
73-11	0.003-0.004	0.4%	Yes, 1290	
73-12	0.0065-0.007		No	700 lbs
73-13	0.008-0.009	Worst bent spec., Not tested		
73-14	0.003-0.004	0.4%	Yes, 1280	
73-15	0.004-0.005	0.3%	No	2200 lbs
73-16	0.002-0.003	0.4%	No	2700 lbs
73-17	0.002-0.003	0.5%	Yes, 506	
73-18	0.004-0.005	0.65%	Yes, 91	
73-19	0.002-0.003	Tensile test	No	
73-20	0.005-0.006	0.3%	Yes, 2700	
73-21	0.004-0.005	0.3%	No	2100 lbs
73-22	0.004-0.005	0.225%	No, 8	
73-23	0.002-0.003	0.2%	No, 9	
73-24	0.004-0.005	0.8%	No	< 1000 lbs
73-25	0.003-0.004	0.2%	Yes, 990484	
73-26	0.002-0.003	0.5%	Yes, 1120	
73-27	0.003-0.004	0.2%	No, 11	
73-28	0.003-0.004	0.2%	Yes, run-out	

Table 3: Summary of the Mechanical Properties

Microstructural Data	Average
ASTM grain size number (MAG=500X):	
The first longitudinal direction (L-T)	11 to 12
(plane perpendicular to applied load)	
Inclusion rating number (MAG=100X):	
Type A (sulfide type), thin series	LT: 1; T-T': 1
Type B (alumina type), thin & heavy series	none
Type C (silicate type), thin & heavy series	none
Type D (globular type), thin & heavy series	LT: thin = 1, heavy = 0.5; T-T': thin = 1, heavy = 0.5
Hardness:	
Brinell (HB)	
Transverse direction (T-T')	665 (converted from HRC)
The first longitudinal direction (L-T)	665 (converted from HRC)
Rockwell B-scale (HRB)	
Transverse direction (T-T')	-
The first longitudinal direction (L-T)	-
Rockwell C-scale (HRC)	
Transverse direction (T-T')	61 (measured)
The first longitudinal direction (L-T)	61 (measured)
Microstructure type:	
Transverse direction (T-T')	martensite
The first longitudinal direction (L-T)	martensite

Monotonic Properties	Average	
Modulus of elasticity, E, GPa (ksi):	207.5	(30,096)
Yield strength (0.2% offset), YS, MPa (ksi):	1275	(185)
Upper yield strength UYS, MPa (ksi):	-	-
Lower yield strength LYS, MPa (ksi):	-	-
Yield point elongation, YPE (%):	-	-
Ultimate strength, S_u, MPa (ksi):	1275	(185)
Percent elongation, %EL (%):	1.0%	
Percent reduction in area, %RA (%):	1.0%	
Strength coefficient, K, MPa (ksi):	2,180.0	(316.2)
Strain hardening exponent, n:	0.0865	
True fracture strength, σ_f, MPa (ksi):	1275	(185)
True fracture ductility, ε_f (%):	0.78%	

Cyclic Properties	Average		Range
Cyclic modulus of elasticity, E', GPa (ksi):	204.2	(29,615)	202.5 - 205.9 (29,362) - (29,868)
Fatigue strength coefficient, σ_f', MPa (ksi):	3,738.8	(542.3)	
Fatigue strength exponent, b:	-0.1906		
Fatigue ductility coefficient, ε_f':	-		
Fatigue ductility exponent, c:	-		
Cyclic yield strength, YS', MPa (ksi)	-		
Cyclic strength coefficient, K', MPa (ksi):	-		
Cyclic strain hardening exponent, n':	-		
Fatigue Limit (defined at 10^6 cycles), MPa (ksi)	235.39	(34.1)	

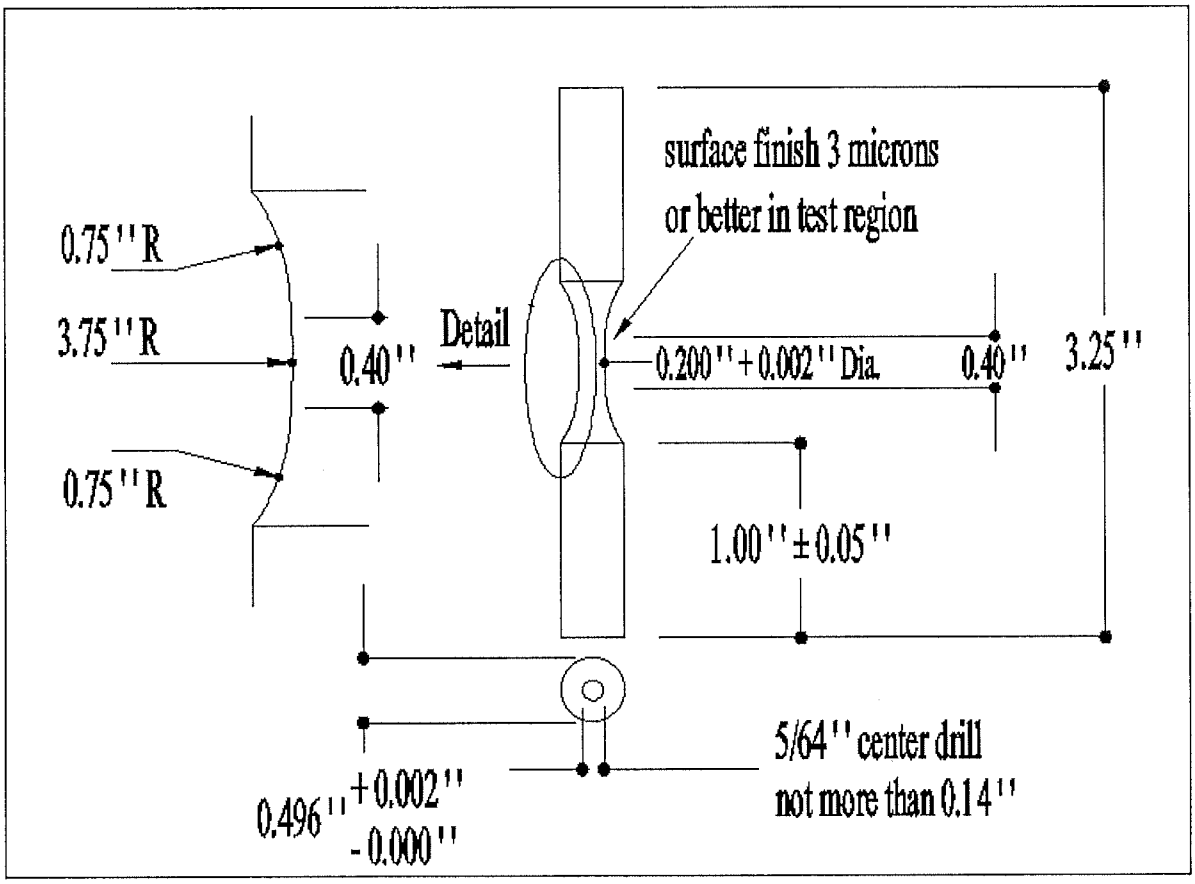

Figure 1: Specimen configuration and dimensions

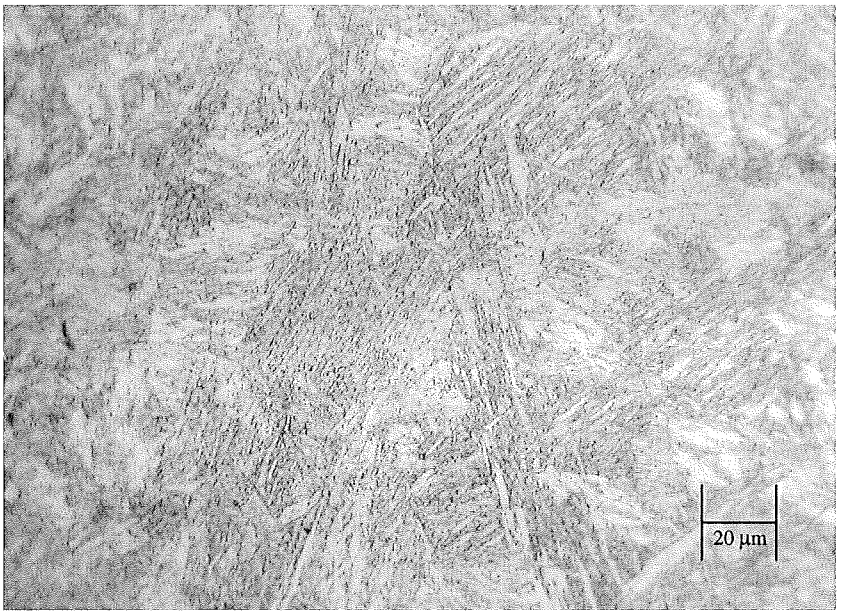

Figure 2: Photomicrograph in the plane perpendicular to the applied load (L-T' direction) at 500X for SAE 41B17M (PS 19) Carburized Case (Atm) steel (rolling direction is perpendicular to the page).

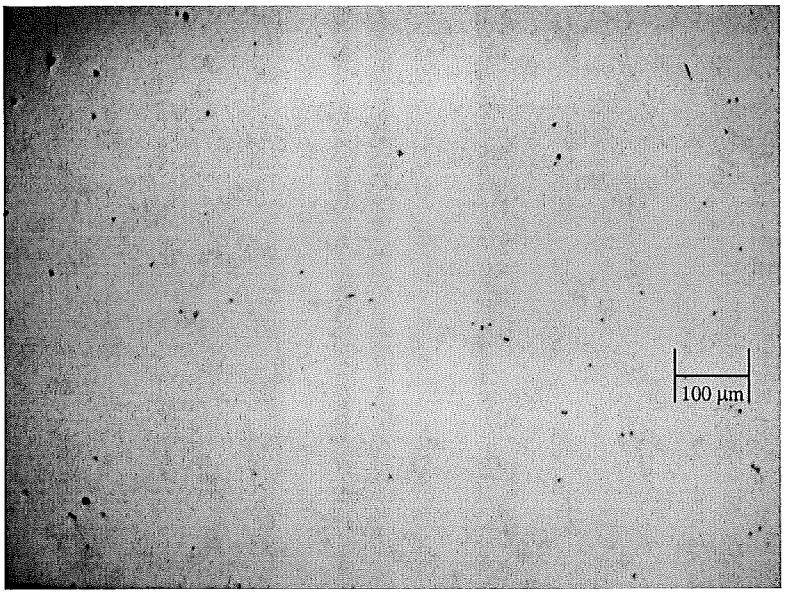

Figure 3 (a): Photomicrograph in the plane perpendicular to the applied load (L-T' direction) at 100X for SAE 41B17M (PS 19) Carburized Case (Atm) steel (rolling direction is perpendicular to the page).

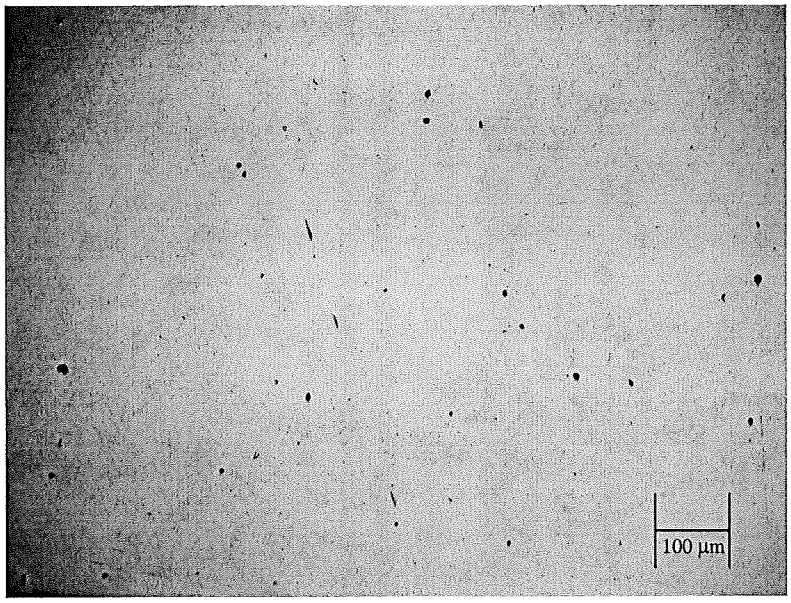

Figure 3 (b): Photomicrograph in the plane perpendicular to the applied load (T-T' direction) at 100X for SAE 41B17M (PS 19) Carburized Case (Atm) steel (rolling direction is parallel to the page).

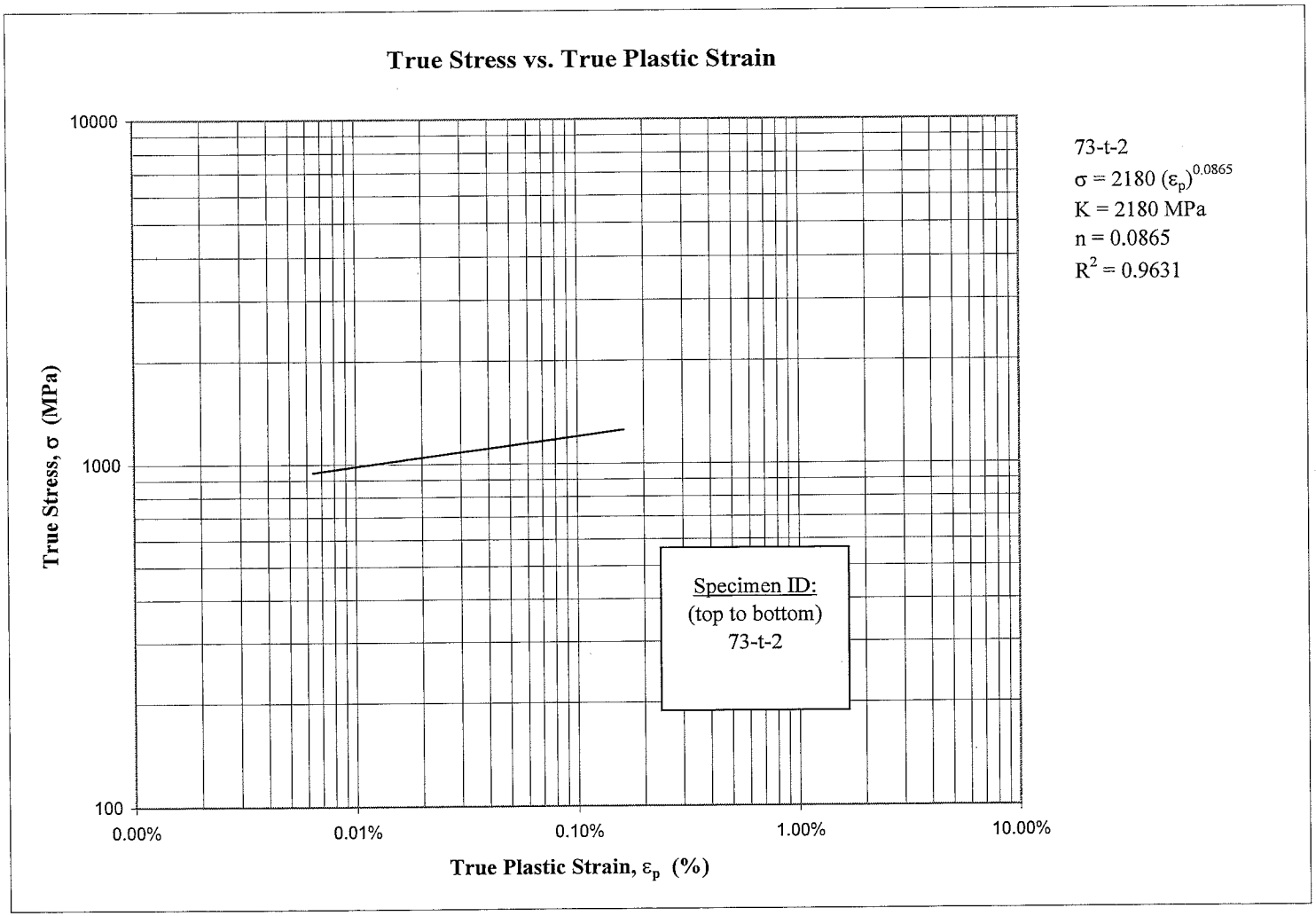

Figure 4: True stress versus true plastic strain

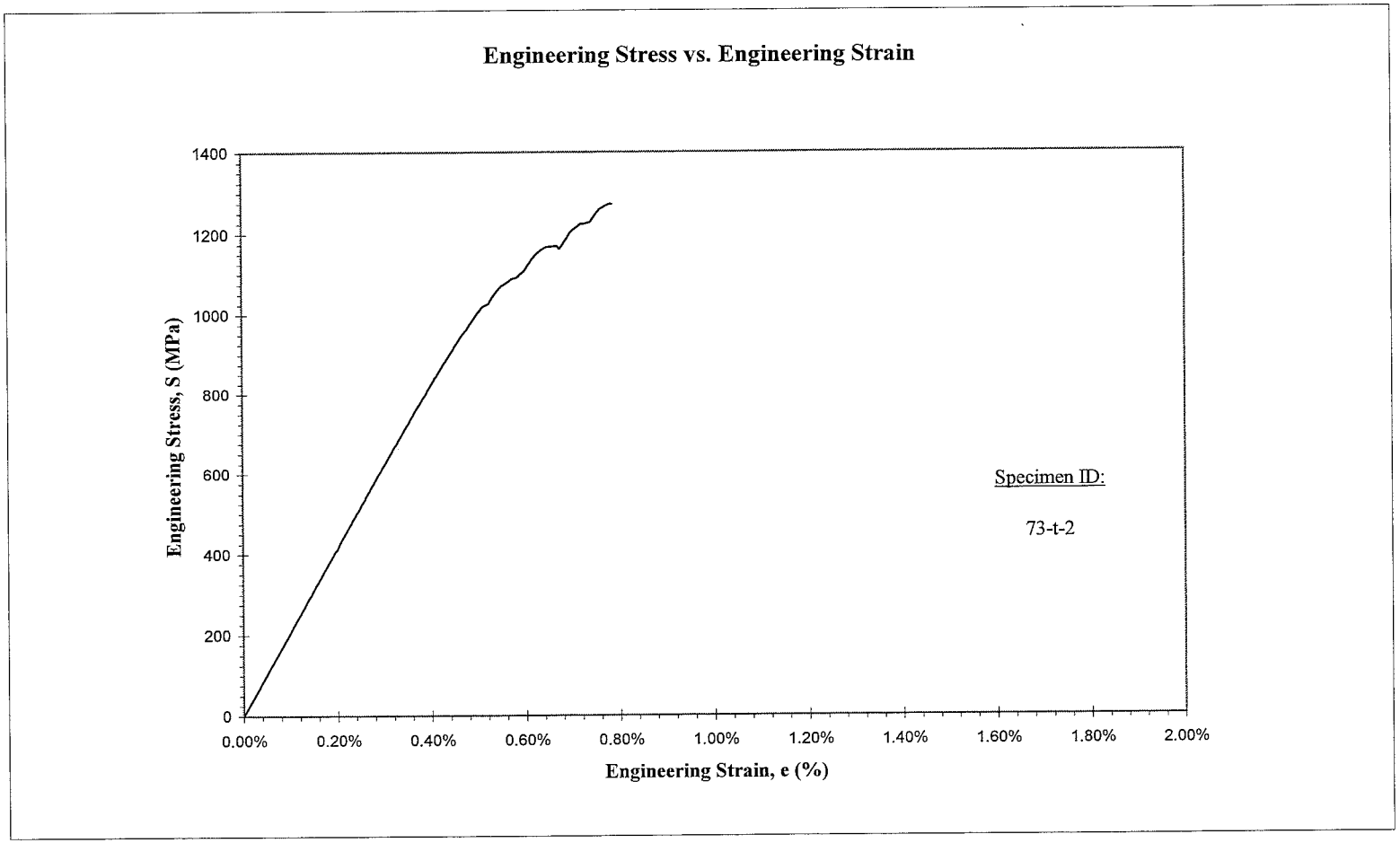

Figure 5: Monotonic stress-strain curve

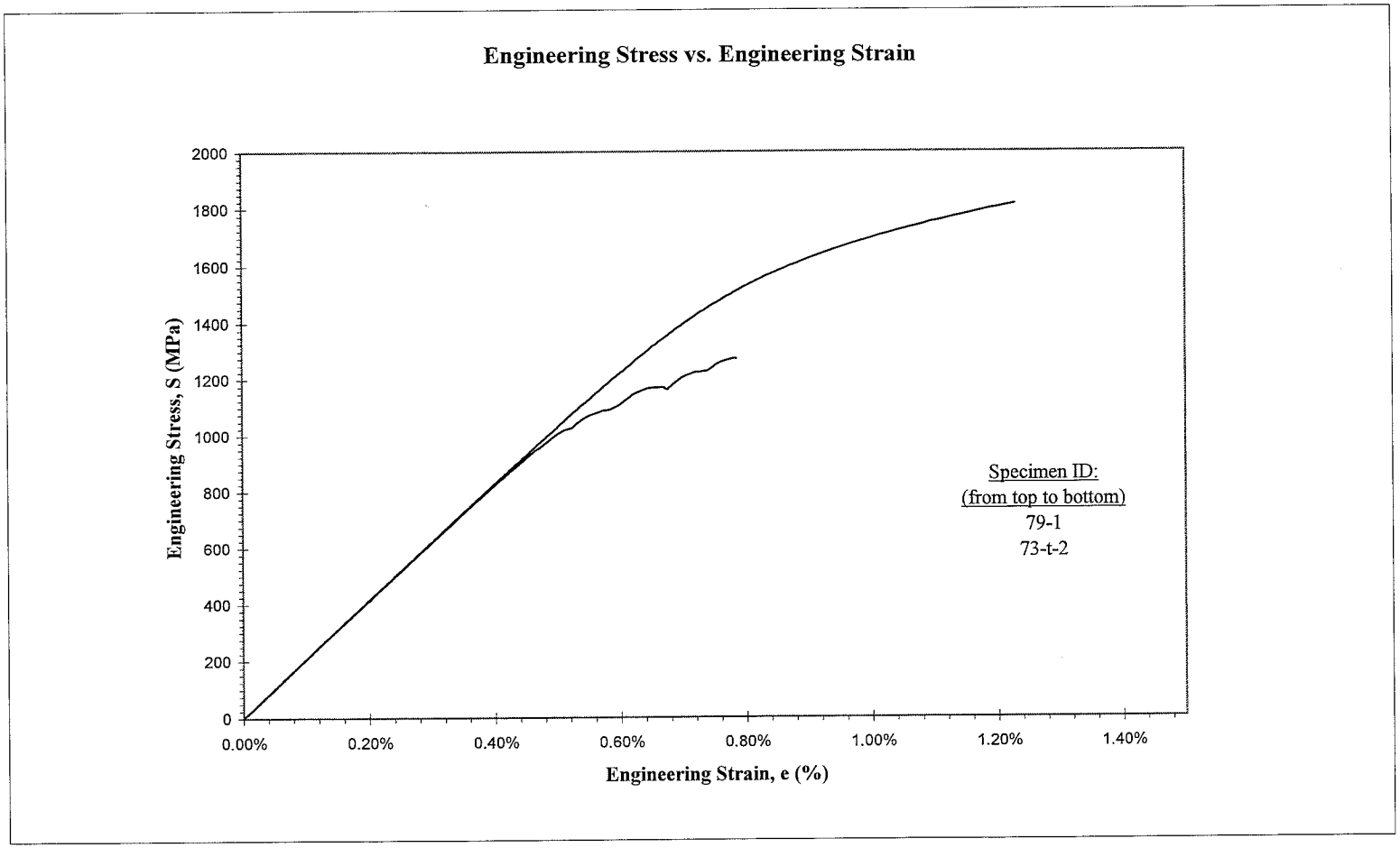

Figure 6: Interposition of monotonic stress-strain curves of iterations 73 and 79

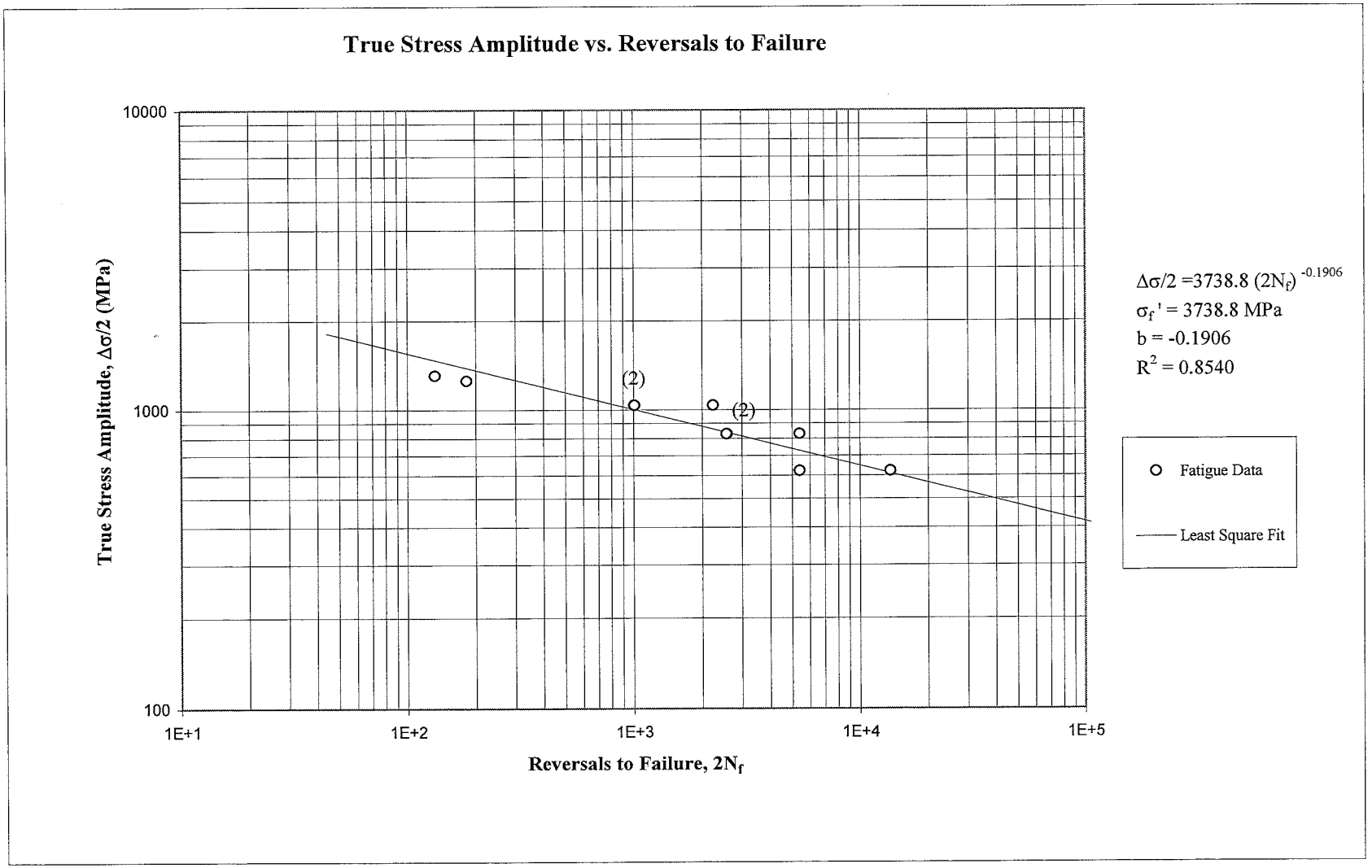

Figure 7: True stress amplitude versus reversals to failure

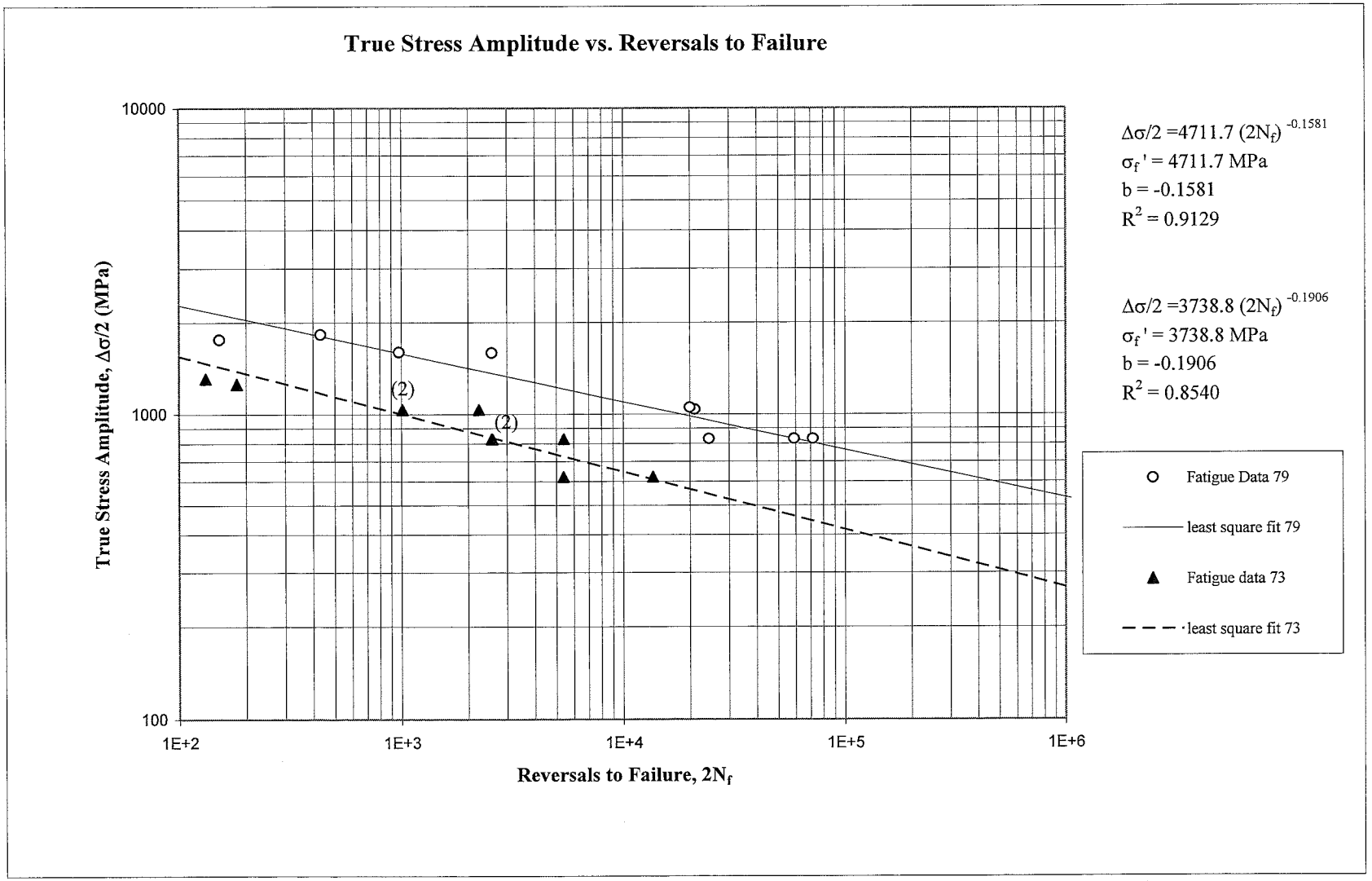

Figure 8: True stress amplitude versus reversals to failure interposition for iterations 73 and 79

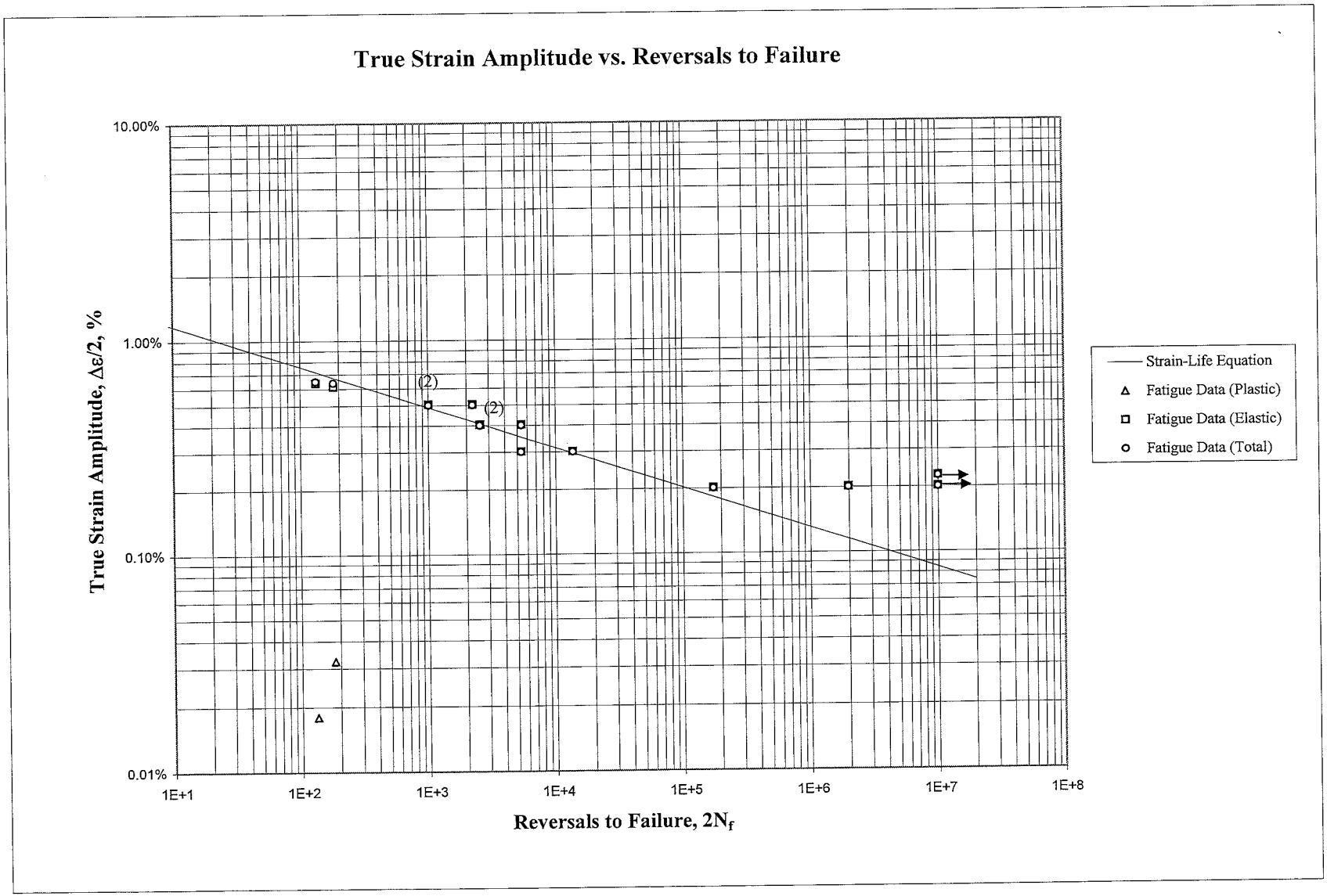

Figure 9: True strain amplitude versus reversals to failure

REFERENCES

[1] ASTM Standard E606-92, "Standard Practice for Strain-Controlled Fatigue Testing," Annual Book of ASTM Standards, Vol. 03.01, 2004, pp. 593-606.

[2] ASTM Standard E83-02, "Standard Practice for Verification and Classification of Extensometers," Annual Book of ASTM Standards, Vol. 03.01, 2004, pp. 232-244.

[3] ASTM Standard E1012-99, "Standard Practice for Verification of Specimen Alignment Under Tensile Loading," Annual Book of ASTM Standards, Vol. 03.01, 2004, pp. 763-770.

[4] ASTM Standard E8-04, "Standard Test Methods for Tension Testing of Metallic Materials," Annual Book of ASTM Standards, Vol. 03.01, 2004, pp. 62-85.

[5] ASTM Standard E112-96, "Standard Test Methods for Determining Average Grain Size," Annual Book of ASTM Standards, Vol. 03.01, 2004, pp. 267-292.

[6] ASTM Standard E45-97, "Standard Test Methods for Determining the Inclusion Content of Steel," Annual Book of ASTM Standards, Vol. 03.01, 2004, pp. 187-199.

[7] ASTM Standard E739-91, "Standard Practice for Statistical Analysis of Linear or Linearized Stress-Life (S-N) and Strain-Life (ε-N) Fatigue Data," Annual Book of ASTM Standards, Vol. 03.01, 1995, pp. 670-676.

[8] ASTM Standard E646-00, "Standard Test Method for Tensile Strain-Hardening Exponents (n-values) of Metallic Sheet Materials," Annual Book of ASTM Standards, Vol. 03.01, 2004, pp. 619-626.

[9] Bridgman, P. W., "Stress Distribution at the Neck of Tension Specimen," *Transactions of American Society for Metals*, Vol. 32, 1944, pp. 553-572.

[10] Stephens R. I., Fatemi A., Stephens R. R. and Fuchs H. O., "*Metal Fatigue in Engineering*", Second edition, Wiley Interscience, 2000.

APPENDIX

Table A.1: Summary of monotonic tensile test results

Specimen ID	D_o, mm (in.)	D_f, mm (in.)	L_o, mm (in.)	L_f, mm (in.)	E, GPa (ksi)	YS (offset=0.14%)*, MPa (ksi)	UYS, MPa (ksi)	LYS, MPa (ksi)	YPE, %	S_u, MPa (ksi)	K, MPa (ksi)	n	%EL, %	%RA, %	R, mm (in.)	σ_f, MPa (ksi)	ε_f
73-t-2	5.05 (0.200)	5.05 (0.199)	7.62 (0.30)	7.70 (0.303)	207.5 (30,095.7)	1274.7 (184.9)	-	-	-	1274.7 (184.9)	2,180.0 (316.2)	0.0865	1%	1%	-	1274.7 (184.9)	0.78%

* As the test did not last upto 0.2% offset, the yield strength was defined at 0.14% offset.

Table A.2: Summary of constant amplitude completely reversed fatigue test results

Specimen ID	Test control mode	Test freq., Hz	E, GPa (ksi)	At midlife ($N_{50\%}$)						$2N_{50\%}$, [a] reversals	$(2N_f)_{50\%}$, [b] reversals	Failure location [c]
				E', GPa (ksi)	$\Delta\varepsilon/2$, %	$\Delta\varepsilon_p/2$ (calculated), %	$\Delta\varepsilon_p/2$ (measured), %	$\Delta\sigma/2$, MPa (ksi)	σ_m, MPa (ksi)			
73-18	strain	0.20	203.2 (29,470)	202.5 (29,362)	0.637%	0.032%	0.018%	1255.4 (182.1)	-258.3 (-37.5)	96	182	IGL
73-3	strain	0.20	205.8 (29,854)	205.9 (29,868)	0.648%	0.018%	0.010%	1307.5 (189.6)	-281.6 (-40.8)	64	132	IGL
73-2	load	0.30	- -	- -	0.500%	-	-	1034.3 (150.0)	0.0 (0.0)	505	1,010	OGIT
73-26	load	0.30	- -	- -	0.500%	-	-	1034.3 (150.0)	0.0 (0.0)	1,120	2,240	IGL
73-17	load	0.30	- -	- -	0.500%	-	-	1034.3 (150.0)	0.0 (0.0)	506	1,012	IGL
73-11	load	0.50	- -	- -	0.400%	-	-	827.4 (120.0)	0.0 (0.0)	1,290	2,580	OGIT
73-14	load	0.50	- -	- -	0.400%	-	-	827.4 (120.0)	0.0 (0.0)	1,280	2,560	IGL
73-9	load	0.50	- -	- -	0.400%	-	-	827.4 (120.0)	0.0 (0.0)	2,702	5,404	IGL
73-4	load	0.75	- -	- -	0.300%	-	-	620.6 (90.0)	0.0 (0.0)	6,817	13,634	OGIT
73-20	load	0.75	- -	- -	0.300%	-	-	620.6 (90.0)	0.0 (0.0)	2,700	5,400	OGIT
73-7	load	1.00 20.00	- -	- -	0.225%	-	-	465.4 (67.5)	0.0 (0.0)	>5,000,000	>10,000,000	No Failure
73-25	load	1.00 25.00	- -	- -	0.200%	-	-	413.7 (60.0)	0.0 (0.0)	990,484	1,980,968	IGL
73-1	load	1.00 4.00	- -	- -	0.200%	-	-	413.7 (60.0)	0.0 (0.0)	87,000	174,000	OGIT
73-28	load	1.00 25.00	- -	- -	0.200%	-	-	413.7 (60.0)	0.0 (0.0)	>5,000,000	>10,000,000	No Failure

[a] $2N_{50\%}$ is defined as the midlife reversal ;

[b] $2(N_f)_{50\%}$ is defined as reversal of 50% load drop or failure

[c] IGL = inside gage length; OGIT = Outside gage length but inside test section

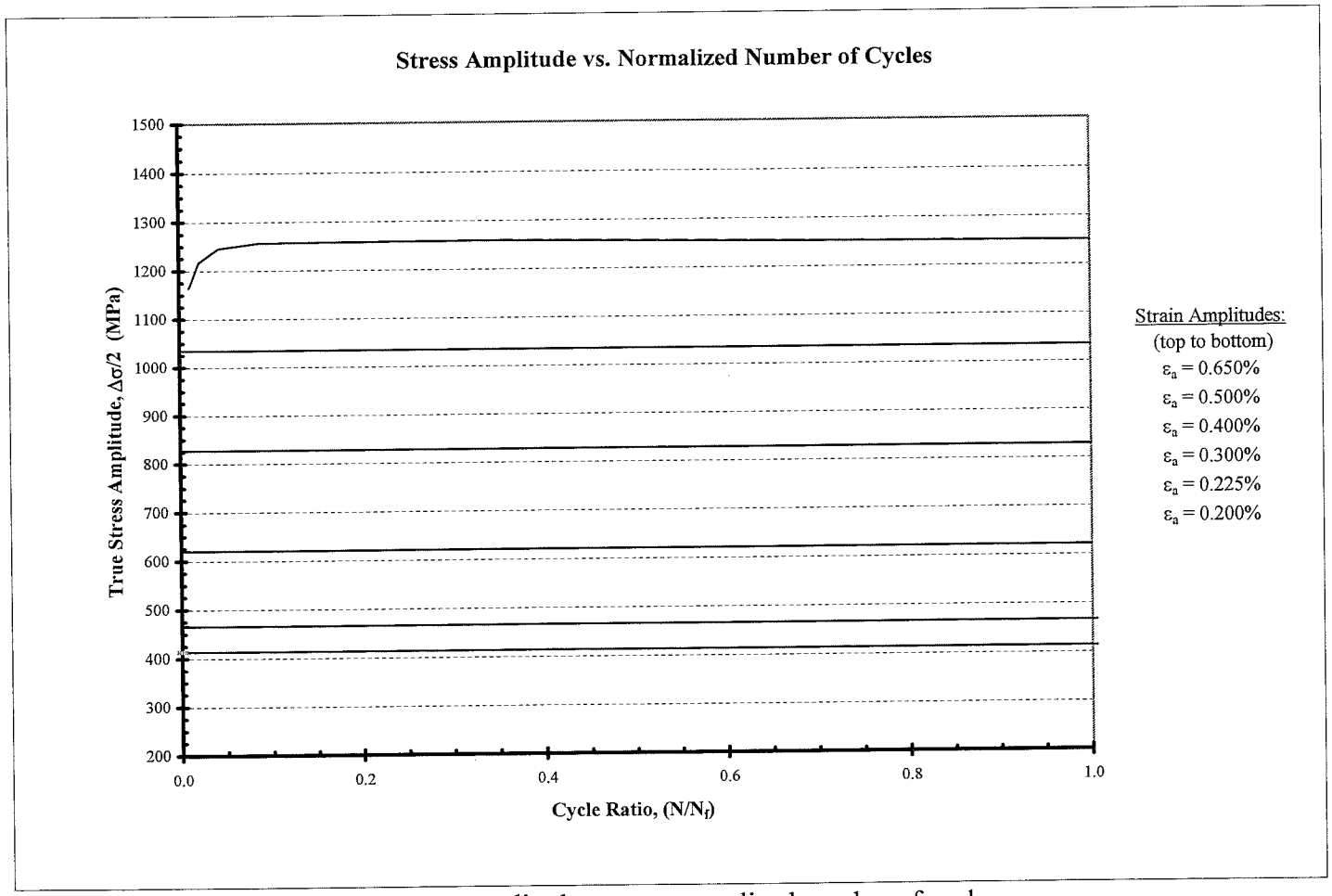

Figure A.1a: True stress amplitude versus normalized number of cycles

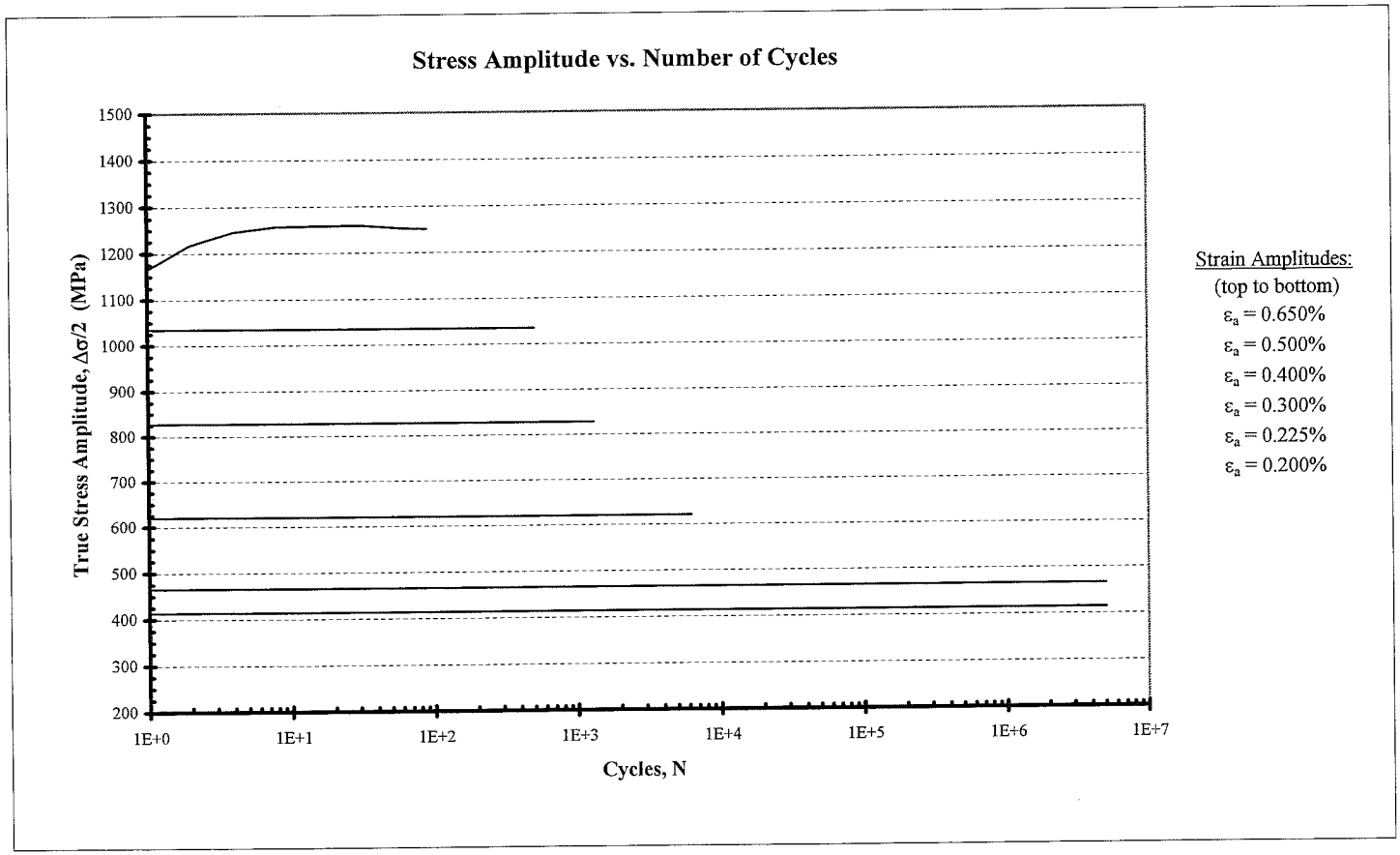

Figure A.1b: True stress amplitude versus number of cycles

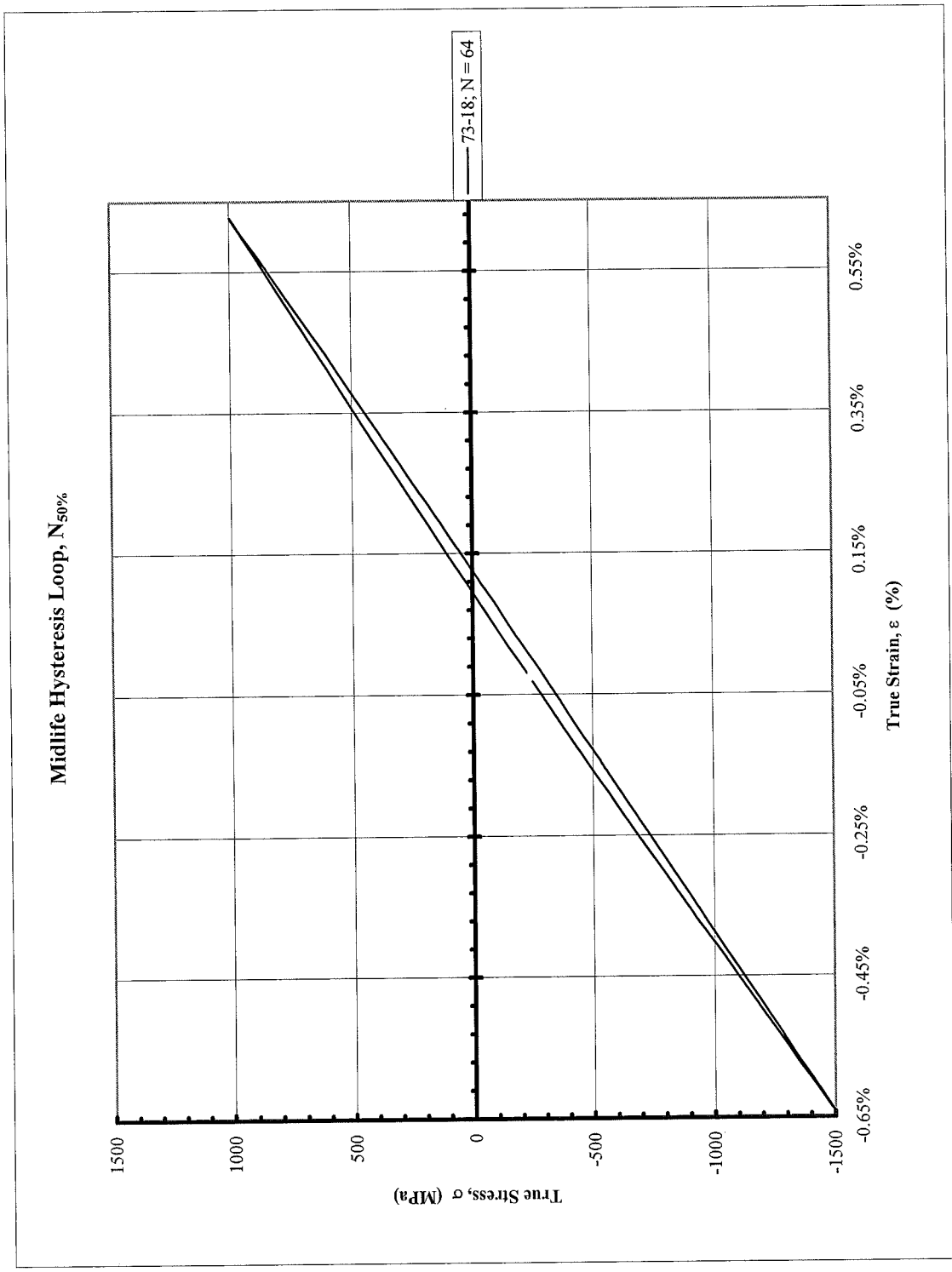

Figure A.2 (a): Midlife hysteresis loop at a strain amplitude of 0.65%

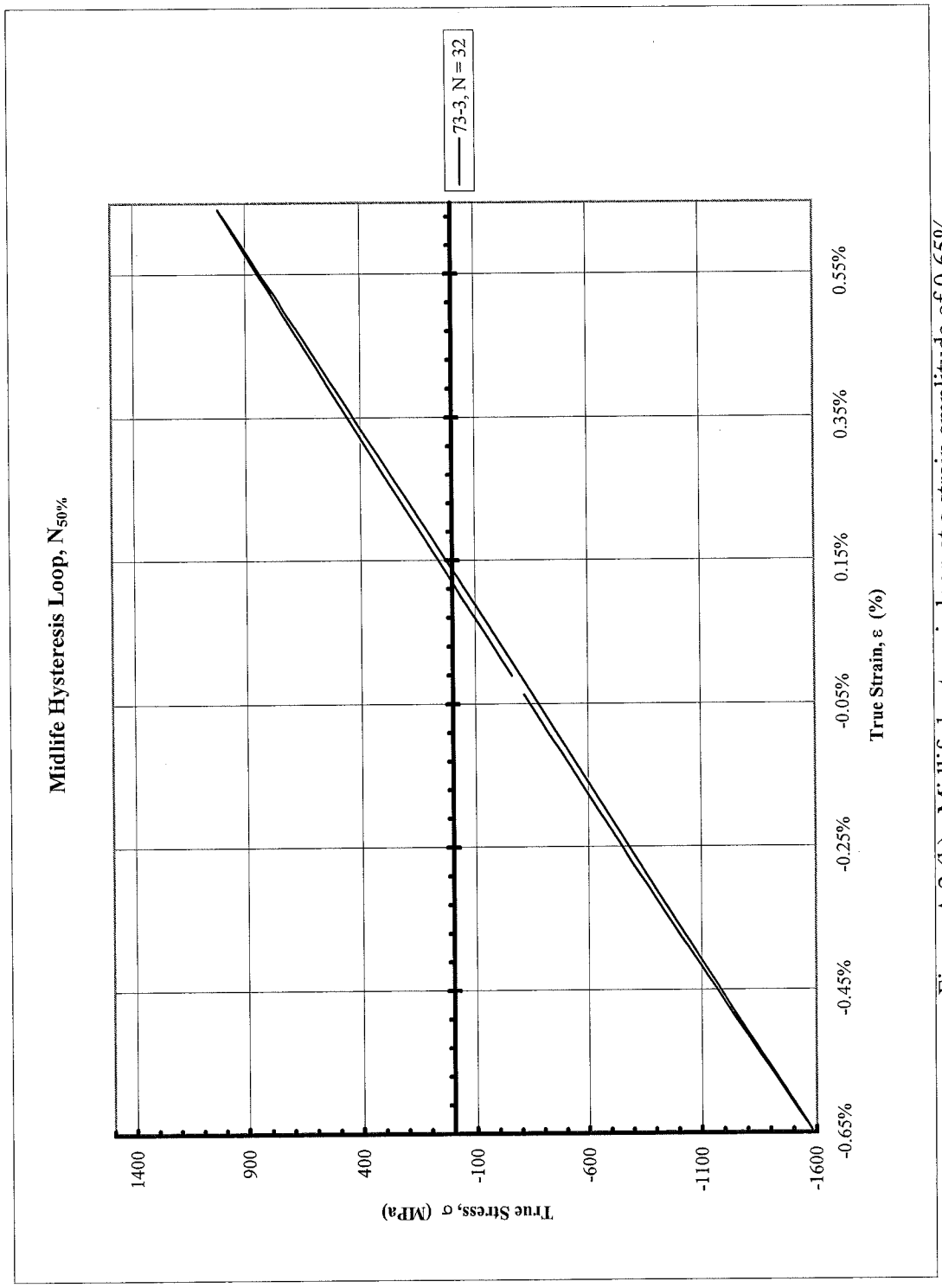

Figure A.2 (b) : Midlife hysteresis loop at a strain amplitude of 0.65%